



HAL
open science

Chiral Anthranyl Trifluoromethyl Alcohols: Structures, Oxidative Dearomatization and Chiroptical Properties

Dorian Sonet, Mattéo Cayla, Raphaël Méreau, Estelle Morvan, Aline Lacoudre, Nicolas Vanthuyne, Muriel Albalat, Dario M Bassani, Antoine Scalabre, Emilie Pouget, et al.

► To cite this version:

Dorian Sonet, Mattéo Cayla, Raphaël Méreau, Estelle Morvan, Aline Lacoudre, et al.. Chiral Anthranyl Trifluoromethyl Alcohols: Structures, Oxidative Dearomatization and Chiroptical Properties. *Chemistry - A European Journal*, 2022, 28 (72), pp.e202202695. 10.1002/chem.202202695 . hal-03961798

HAL Id: hal-03961798

<https://hal.science/hal-03961798>

Submitted on 29 Jan 2023

HAL is a multi-disciplinary open access archive for the deposit and dissemination of scientific research documents, whether they are published or not. The documents may come from teaching and research institutions in France or abroad, or from public or private research centers.

L'archive ouverte pluridisciplinaire **HAL**, est destinée au dépôt et à la diffusion de documents scientifiques de niveau recherche, publiés ou non, émanant des établissements d'enseignement et de recherche français ou étrangers, des laboratoires publics ou privés.

Chiral Anthranyl Trifluoromethyl Alcohols: Structures, Oxidative Dearomatization and Chiroptical Properties

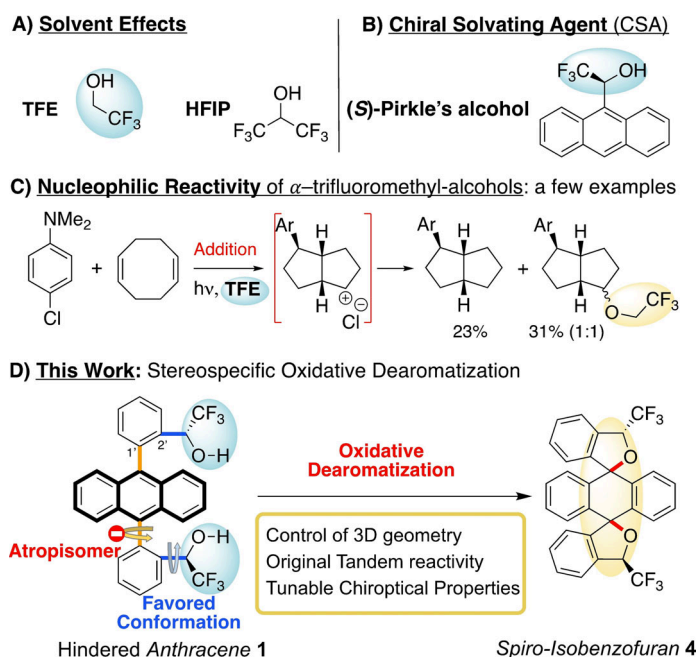
Dorian Sonet,^[a] Mattéo Cayla,^[a] Raphaël Méreau,^[a] Estelle Morvan,^[b] Aline Lacoudre,^[a] Nicolas Vanthuyne,^[c] Muriel Albalat,^[c] Dario M. Bassani,^[a] Antoine Scalabre,^[d] Emilie Pouget,^[d] and Brigitte Bibal*^[a]

Abstract: Chiral trifluoromethyl alcohol groups were introduced at the hindered *ortho* positions of 9,10-diphenylanthracenes to investigate their effects on the physical properties and reactivity towards oxidative dearomatization. In such compact structures, the position in different quadrants and the preferred orientation of the $-\text{CH}(\text{OH})\text{CF}_3$ groups were determined by the relative and absolute configurations of each stereoisomer, respectively. As a consequence, the stereochemistry governs the organization of the H-bonded

molecules in single crystals (homochiral dimers vs ribbon), whereas in chlorinated solvents, they all behave as discrete compounds. Concerning their reactivity, the stereospecific dearomative oxidation of these molecules leads to 9,10-bispiro-isobenzofuran-anthracenes, when using organic single-electron transfer oxidants. The chiroptical properties of the alcohols and the corresponding dearomatized products were compared and showed an important modulation of the intensity.

Introduction

α -Trifluoromethyl alcohols represent a well-known class of compounds exploited for their physical organic properties owing to their high polarity and ionizing power, mild acidity (pK_a similar to phenols), strong hydrogen bond donor/poor acceptor groups and low chemical reactivity.^[1,2] Compared to their hexafluorinated homologues such as hexafluoroisopropanol (HFIP), α -trifluoromethyl alcohols offer the advantage of less extreme properties, such as a moderate steric hindrance that facilitates their incorporation into organic architectures (Figure 1).^[3,4] Concerning their applicability, α -trifluoromethyl alcohols have amphiphilic properties that are exploited by the pharmaceutical industry to enhance the drug availability or activity (befloxatone, LX-301).^[5] The H-bond donor properties of $\text{RCH}(\text{OH})\text{CF}_3$ molecules were initially exploited within chiral



[a] D. Sonet, M. Cayla, Dr. R. Méreau, A. Lacoudre, Dr. D. M. Bassani, Prof. Dr. B. Bibal
Institut des Sciences Moléculaires UMR CNRS 5255
Univ. Bordeaux, CNRS, Bordeaux INP
351 cours de la Libération, 33400 Talence (France)
E-mail: brigitte.bibal@u-bordeaux.fr

[b] E. Morvan
Institut Européen de Chimie et Biologie UAR3033 CNRS
University of Bordeaux, INSERM US001
2 rue Roger Escarpit, 33607 Pessac (France)

[c] Dr. N. Vanthuyne, M. Albalat
Centrale Marseille, iSm2, Aix-Marseille Université, CNRS
52 avenue Escadrille Normandie Niemen, 13013 Marseille (France)

[d] Dr. A. Scalabre, Dr. E. Pouget
Chimie et Biologie des Membranes et des Nanoobjets
UMR CNRS 5248, Université de Bordeaux
2 rue Roger Escarpit, 33607 Pessac (France)

Figure 1. α -Trifluoromethyl alcohols A) as solvents in organic synthesis, B) as chiral solvating agents in analytical chemistry, C) as nucleophiles in a few cases, and D) within hindered chiral architectures 1 to explore their preorganization and unusual oxidative dearomatization into isobenzofurans 4. The chiroptical properties of 1 and 4 were also examined.

solvating agents, such as Pirkle's alcohol, for the determination of the enantiomeric excess (Figure 1B).^[6]

2,2,2-Trifluoroethanol (TFE, Figure 1A) is widely employed as a solvent or an additive in organic synthesis to optimize different reactions: (photo)oxidations, nucleophilic substitutions and additions, cycloadditions, electrophilic and dearomative reactions.^[1-3] On the other hand, the nucleophilic reactivity of α -

trifluoromethyl alcohols is far less documented. For TFE, some tandem nucleophilic addition reactions^[7] on aromatic or aliphatic carbocations were reported to have poor stereoselectivity whereas nucleophilic substitutions^[8] on carbohydrates^[9] via an oxocarbenium intermediate were stereoselective (Figure 1C).

Beyond the successful example of TFE, few trifluoromethyl^[6,10–13] or hexafluoromethyl^[14] alcohol groups were implemented on more elaborated skeletons, possibly due to self-aggregation issues that may limit their benefit.^[15] In addition, the control of the non-symmetric induction (i.e., the diastereoisomers are obtained in a non statistical ratio, without any asymmetric induction) and the nucleophilicity of the α -trifluoromethyl alcohol group have received little attention.

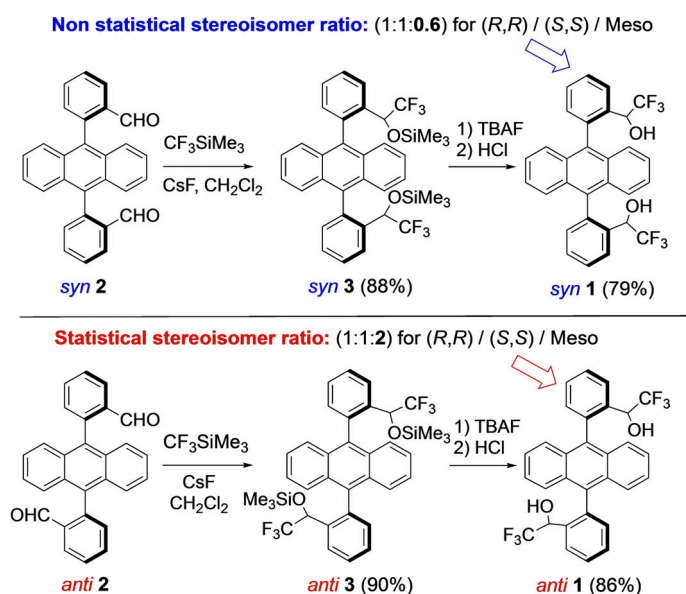
To further explore the physical properties and the reactivity of chiral α -trifluoromethyl alcohols, we envisioned to implement this functional group on 9,10-diphenylanthracenes (DPA) by preparing compounds **1** (Figure 1D) which present two hindered groups on adjacent carbons C1' and C2'. Belonging to the class of chiral atropisomers,^[16] compounds **1** exist as *syn* and *anti* isomers due to the locked rotation along the C₁'-Ar-C₉-anthryl bond. In this environment, the rotation of the vicinal C₂'-Ar-C_{H(OH)CF₃} bonds may be either restricted (rotamers) or orientated by electronic factors (favored conformers).^[6d] Firstly, the structural properties of architectures **1** were investigated by NMR, X-ray diffraction and molecular modeling. Secondly, the oxidative dearomatization of anthracenes **1** into spiro-benzofuranes **4** was achieved through the synergistic oxidation of anthracene^[17] and the nucleophilic addition of CH(OH)CF₃ moieties. This pathway for the dearomatization of anthracenes is novel compared to the classical [4+2] cyclo-additions, metal-catalyzed or organolithium additions.^[18] In addition, this access to chiral fluorinated spiro-heterocycles is a new route, complementary to the rare examples of fluoro-spirocyclizations^[19,20] and post-fluorination of spirocycles.^[21,22] Thirdly, the chiroptical properties of enantiopure compounds **1** and **4** was investigated and compared. The variation of chiroptical properties by an oxidative stimulus can be attractive and less demanding in synthetic efforts compared to the classical approaches, that is, the synthesis of compounds series or the preparation of more sophisticated molecules.^[23,24]

Results and Discussion

Synthesis of fluorinated alcohols

Syn and *anti* atropisomers **1** were obtained by using a two-step pathway from 9,10-bis(2-formylphenyl)-anthracene^[25] *syn*- and *anti*-**2**, respectively. The retention of relative configuration along the synthesis was expected due to the high rotational barrier for *ortho,ortho'*-disubstituted 9,10-diphenyl anthracenes.^[26–27]

The functionalization of each dialdehyde *syn*-**2** or *anti*-**2** was independently conducted in the presence of the nucleophilic Prakash-Ruppert's reagent (2.3 equiv.) to create two asymmetric carbons (Scheme 1). The resulting bis-(α -trifluorometh-



Scheme 1. The two-step synthesis of chiral *ortho,ortho'*-(α -trifluoromethyl)alcohols implemented on *syn*- and *anti*-9,10-diphenylanthracenes **1**. A nonsymmetric induction is observed for *syn*-**1**.

yl)trimethylsilyl ethers *syn*-**3** (88% yield) and *anti*-**3** (90% yield) were isolated in high yields, as a mixture of stereoisomers that were separated at the following step. Finally the deprotection of each rotamer **3** with TBAF independently afforded bis-(α -trifluoromethyl)alcohols *syn*-**1** (89% yield) and *anti*-**1** (93% yield) respectively. The purification of these compounds **1** on column chromatography on silica gel allowed the separation of the *meso* *R,S* diastereoisomer from the racemic mixture of *R,R/S,S* compounds.

Interestingly, the stereoisomeric ratios for products **1** depend on the relative (*syn* or *anti*) configuration of the starting material **2** (Scheme 1). *Anti*-**1** was obtained as a quasi statistical ratio of stereoisomers, that is, 47% of the racemic *R,R/S,S* compound ((\pm)-*anti*-**1**) and 46% of the (*R,S*)-*meso-anti*-**1** instead *syn*-**1** was isolated as 69% of racemic *R,R/S,S* mixture (named (\pm)-*syn*-**1**) and only 20% of the *R,S meso* compound. This nonsymmetric induction revealed in the last step obviously occurred during the second step when the aldehyde *syn*-**2** undergoes a double nucleophilic addition of the trifluoromethyl carbanion. Indeed, the addition of the first equivalent of the Prakash's reagent results in the anchorage of a bulky (α -trifluoromethyl)trimethylsilyl ether group close to the remaining aldehyde function which probably accounts for this nonsymmetric induction observed on the *syn*-products **1** and not on *anti*-**1**.

Racemic and *meso* stereoisomers of both *syn*- and *anti*-**1** were fully characterized. As expected from their structural differences, the *syn* and *anti* relative configurations that respectively place the -CH(OH)CF₃ groups in close proximity or on opposite half-spaces with respect to the anthracene core, have an impact on the physical properties of compounds. For instance, all stereoisomers of *syn*-**1** are fully soluble in chlorinated solvents whereas those of *anti*-**1** are only partially soluble. The melting point of each diastereoisomer **1** was

different: 218 °C for (\pm)-*syn*-1, 227 °C for *meso*-*syn*-1, 345 °C for (\pm)-*anti*-1 and 349 °C for *meso*-*anti*-1. These large differences between *syn*- and *anti*-1 could be attributed to the nature of H-bonded networks in solution and in the solid state that will be disclosed below.

DFT calculations at the M06-2X/6-311G(d,p) level of theory concerning the rotation of the C_{sp^2} - C_{sp^2} bond (Figure 1, blue arrow) indicated that the *syn/anti* relative configurations are very stable with a high rotational barrier of 41.3 kcal mol⁻¹ for *syn*-1 and 43.2 kcal mol⁻¹ for *anti*-1 (see the Supporting Information). This theoretical result corroborates the thermal stability we observed when heating neat compounds 1 at 110 °C for 12 h without any structural modification.

Finally, racemic mixtures of *syn*- and *anti*-1 were separated by chiral HPLC allowing the obtention of the four chiral stereoisomers with excellent enantiomeric excess (*ee*) in the range of 97.5–99.5% and very good yields: (*R,R*)-*syn*-1 in 31% yield, (*S,S*)-*syn*-1 in 28% yield, (*R,R*)-*anti*-1 and (*S,S*)-*anti*-1 both in 20% yield.

H-bonded atropisomers in the solid state

A few crystallographic structures of chiral (α -trifluoromethyl)alcohols are known.^[28] Pioneering work of Berkessel pointed out that the racemic mixture of (α -trifluoromethyl)alcohols containing a ketone group crystallized as heterochiral dimers whereas the *S* enantiomer preferentially forms as zigzag ribbons. Herein we present the first example of bis-(α -trifluoromethyl)alcohols whose structures in the solid state are controlled by both relative and absolute configurations.

The *syn/anti* relative and the absolute configurations of stereoisomers 1 were unambiguously determined by X-ray diffraction on single crystals of (\pm)-*syn*-1, *meso*-*syn*-1, (\pm)-*anti*-1 and *meso*-*anti*-1.

Firstly, the single crystals were grown in non-competitive H-bonding solvents, by the slow diffusion of pentane into a solution of 1 in dichloromethane. Interestingly, the α -trifluoromethyl alcohols self-assemble through strong intermolecular H-bonds between the alcohol groups (distance H–O...H inferior to 2.01 Å). In addition, the nature of the H-bonding assemblies depends on the relative configuration: *meso* and racemic *syn*-1 form dimers (Figure 2a) whereas *meso*-*anti*-1 is organized as oligomers in the solid state (Figure 2b).

It is noteworthy that the crystallization of racemic *syn*-1 led to the co-crystallization of (*R,R*)- and (*S,S*)-*syn*-1 as self-sorted homochiral dimers: ((*R,R*)-*syn*-1)₂ and ((*S,S*)-*syn*-1)₂ (Figure 2a). This homochiral self-sorting observed by crystallization was also confirmed by molecular modeling for H-bonded dimer *syn*-1 (see the Supporting Information).

Secondly, due to their low solubility in apolar solvents, single crystals of *anti*-1 were also grown in dichloromethane with two drops of a H-bond-accepting solvent. Then, the crystallographic structures of (\pm)-*anti*-1.3(DMSO) and *meso*-*anti*-1.1(CH₃COCH₃) were obtained without any self-assembly of anthracene moieties. In these cases, isolated molecules of 1 presented strong H-bonds between the alcohol groups and

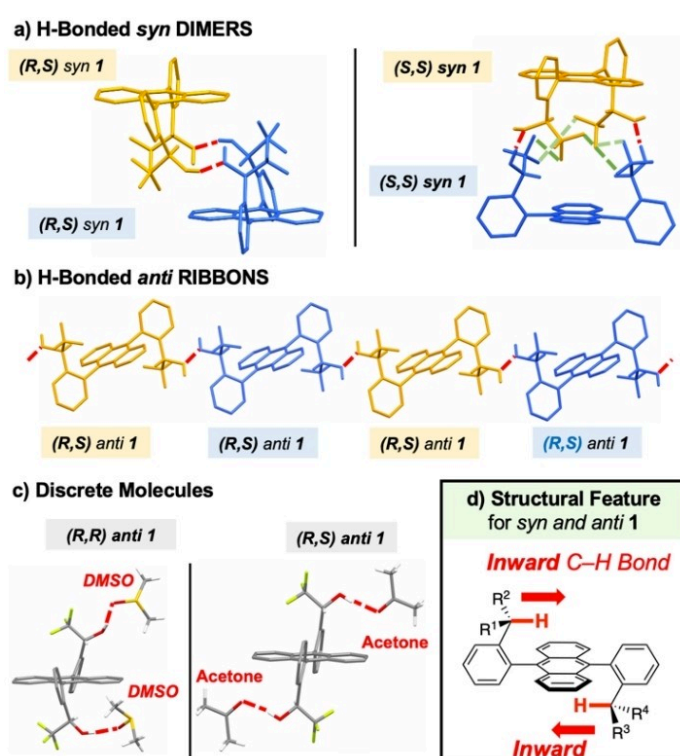


Figure 2. Solid-state structures of *syn*- and *anti*-1 determined by X-ray diffraction showing H-bonded associations. a) *Meso*-*syn*-1 is organized as a dimer with off-set anthracene moieties, whereas (\pm)-*syn*-1 forms homochiral dimers with anthranil moieties shifted by 60°. b) *Meso*-*anti*-1 is arranged as H-bonded ribbons. c) In the presence of H-bond-donor solvents, the crystal structures are individual compounds (shown racemic and *meso*-*anti*-1). d) A systematic positioning of the –CH(OH)CF₃ group with the C_{sp^2} -H pointing towards the anthracene core is observed in all crystals (only *anti*-1 is represented).

DMSO (distance H–O...O=S is 1.77–1.81 Å) or acetone (distance H–O...O=C is 1.94 Å) molecules, respectively (Figure 2d).

All crystallographic structures of atropisomers 1 have a common structural feature for the –CH(OH)CF₃ groups whatever the H-bonding network: each asymmetric carbon has a preferred arrangement in which the C_{sp^3} -H bond is directed towards the anthracene core and thus presents less steric hindrance to the proximal bulky OH and CF₃ substituents, that seat above the 1,8 and 4,5 positions of anthracene (Figure 2d). This particular arrangement of –CH(OH)CF₃ groups of 1 in solution is discussed below.

Hydrogen-bonded atropisomers in solution

To investigate the structure and the H-bonding behavior of compounds *syn*- and *anti*-1 in solution, 1D and 2D NMR experiments were performed on the different atropisomers.

Diffusion-ordered spectroscopy (DOSY) experiments were conducted on atropisomers *syn*- and (\pm)-*anti*-1 (1 mM) in CD₂Cl₂ and indicated similar diffusion coefficients (*D*) of 1.00–1.03 × 10⁻⁹ m²s⁻¹ (Table 1).^[29] Using the Stokes–Einstein equation, the calculated hydrodynamic volumes *V*_H were found to be in the

Table 1. DOSY experiments and comparison between measured diffusion constants (D),^[a] the calculated hydrodynamic volumes (V_H) and estimated volumes ($V_{X\text{-ray}}$) from X-ray structures for atropisomers **1**.

	D [$\times 10^{-9}$ m ² s ⁻¹]	V_H [\AA^3]	$V_{X\text{-ray}}$ [\AA^3] single/dimer ^[b]
(\pm)- <i>syn</i> - 1	1.03 (CD ₂ Cl ₂)	550	530/1350
(<i>R,S</i>)- <i>syn</i> - 1	1.00 (CD ₂ Cl ₂)	600	530/1150
(\pm)- <i>anti</i> - 1	1.02 (CD ₂ Cl ₂)	566	600/n.d. ^[c]
(<i>R,S</i>)- <i>anti</i> - 1	0.171 ([D ₆]DMSO)	830	600/3800

[a] Diffusion-ordered spectroscopy experiments (DOSY) were conducted on compounds **1** (1 mM) in deuterated dichloromethane or DMSO at 25 °C. [b] Calculated volumes for a single compound and the corresponding H-bonded dimer. [c] Not determined.

range of 550–600 \AA^3 , which correspond to the volume of single molecules based on X-ray data ($V_{X\text{-ray}} = 530\text{--}600 \text{\AA}^3$).

Concerning *meso-anti*-**1** which was only soluble in [D₆]DMSO, the calculated hydrodynamic V_H in this solvent was slightly larger (830 \AA^3) but was still in a good agreement with the volume occupied by a single molecule in the solid state compared to a H-bonded dimer (ca. 3800 \AA^3).

In contrast to their behavior in the solid state, DOSY experiments clearly reveal that (\pm)-*syn*, *meso-syn*- and (\pm)-*anti*-**1** at a concentration of 1 mM are not aggregated in CD₂Cl₂, an apolar aprotic solvent. This result is in line with the description of chiral (poly)fluorinated alcohols in which H-bonding behavior differs between solution and the solid state.^[14a]

Variable temperature ¹H NMR spectroscopy of racemic mixtures of *syn*- and *anti*-**1** (2 mM, C₂D₂Cl₄) between 20 and 105 °C evidenced no changes in spectra, except complexation/decomplexation of residual water molecules (see the Supporting Information). Along with the lack of any concentration dependence (0.2–10 mM, CDCl₃), this strongly suggests that **1** is present as discrete molecules in chlorinated solvents.

Solvation effects for racemic *syn*- and *anti*-**1** were noticeable in the ¹H NMR spectra (see the Supporting Information). In particular, a marked anisochrony is seen for the aromatic protons when employing [D₈]toluene or chlorinated solvents (Figure 3). In C₂D₂Cl₄, the anthracene protons of (\pm)-*syn*-**1** appeared as four distinct signals (H₁/H₅, H₄/H₈, H₃/H₇ and H₂/H₆) between 7.6 and 7.4 ppm, meanwhile those of less hindered dialdehyde *syn*-**2** were characteristics of 9,10-substituted an-

thracenes with two sets (dd) at 7.5 ppm (central protons H_{1,4,5,8}) and at 7.4 ppm (peripheral protons H_{2,3,6,7}).

1D or 2D ¹H,¹⁹F heteronuclear Overhauser effect spectroscopy (HOESY)^[30] experiments conducted in CD₂Cl₂ confirmed the spatial proximity of the CF₃ groups to two specific anthracene protons depending on each stereoisomer. In the case of (\pm)-*syn*-**1**, the fluorine atoms were close to the H₁ and H₅ protons, without any proximity to the symmetric H₄ and H₈ protons (Figure 3). The ¹H,¹⁹F HOESY analysis conducted on *meso-syn*-**1**, (\pm)-*anti*-**1** and *meso-anti*-**1** confirmed a similar specific anisotropy of the anthracene aromatic protons. However, these analyses conducted at 20 °C cannot rule out neither a restricted rotation of the C_{sp³}–C_{sp²} bond nor a preferred conformation^[6d,31] for the fluorinated group.

DFT calculations were carried out on **1** to consider the rotation of the C_{sp³}–C_{sp²} bond. As the rotational barriers for the C_{sp³}–C_{sp²} bond were found to be moderate for *syn*-**1** (9.4 kcal.mol⁻¹) and *anti*-**1** (9.0 kcal.mol⁻¹), these can be interpreted as free rotors. Among the optimized conformers for each stereoisomer, the more stable one consistently present a C_{sp³}–H bond pointing towards the anthracene group (Figure 2d) and is the major one by far, according to the Boltzmann populations: 83% for (*S,S*)-*syn*-**1**, 94% for (*R,S*)-*syn*-**1** and 99% for (*S,S*)-*anti*-**1**.

Notably, the latter *syn* structures do not favor any intramolecular H-bonds. The molecular modeling indicates a preferred orientation of each –CH(OH)CF₃ groups within atropisomers **1**, with the C_{sp³}–H bond pointing inwards, probably due to electronic factors.

According to NMR studies, *syn*- and *anti*-atropisomers **1** behave as isolated molecules in CD₂Cl₂, without self-associations. NMR and DFT calculations strongly suggest that the –CH(OH)CF₃ asymmetric carbons adopt a preferred conformation (C–H bond directed inwards, Figure 2d), that consequently positions the CF₃ groups in a precise quarter space depending on the relative and absolute configurations of each compound **1**.

Controlled tandem reactivity

The dearomatization reactions of nonactivated arenes are of particular interest as these transformations provide complex and value-added compounds from cheap starting materials.^[18,32] Concerning anthracene and 9,10-disubstituted anthracenes, the classical routes to their dearomatization (Scheme 2A and C) are either cycloadditions^[33] or tandem reactions such as the nucleophilic dearomatization reaction^[34,35] that consists of a nucleophilic addition on the arene followed by an electrophilic quench.

Concerning hindered 9,10-diphenylanthracenes, their dearomatization is mainly reported using a regioselective [4 + 2] cycloaddition with singlet oxygen on the 9,10 positions (Scheme 2C). To the best of our knowledge, an alternative oxidative dearomatization of 9,10-diphenylanthracenes has not been reported. We envisioned that the two-electrons oxidation of the anthracene core in **1** can provide two electrophilic sites

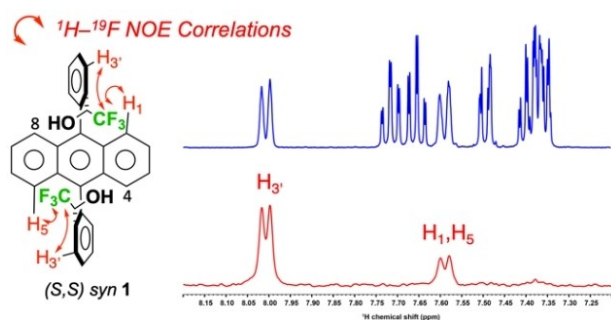
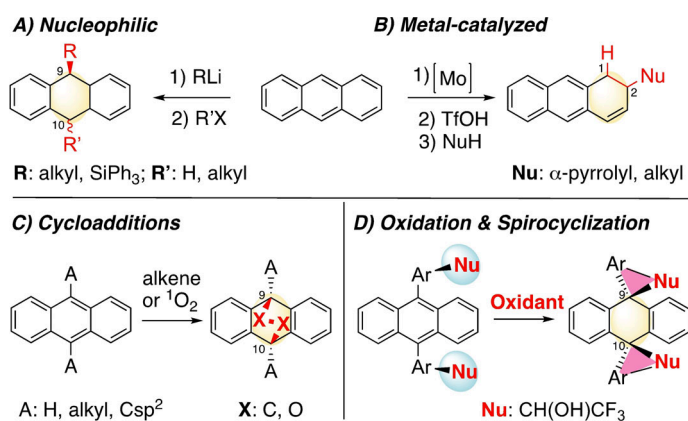


Figure 3. Left: structure of (*S,S*)-*syn*-**1** with the ¹H,¹⁹F NOE correlations; right: aromatic region of the 1D (blue) and 1D selective ¹H,¹⁹F HOESY (red) NMR spectra of (\pm)-*syn*-**1** (400 MHz, CD₂Cl₂, 2 mM).



Scheme 2. Routes for the dearomatization of anthracenes. a) Nucleophilic dearomatization followed by an electrophilic quench, b) acid/nucleophile tandem additions catalyzed by molybdenum, c) [4 + 2] cycloadditions with dienophiles, and d) the new access through a tandem oxidation/spirocyclization reaction when 9,10-diaryl anthracene possesses α-trifluoromethyl alcohol substituents in *ortho*' positions.

on the C-9 and C-10 positions, which may then intramolecularly react with the fluorinated alcohol groups, possibly leading to dearomatized bis-spirocyclic compounds **4** whose stereochemistry could be controlled by a “*syn/anti* atropisomeric lock” (Scheme 2D, Table 2).

Control experiments conducted using light activation revealed that anthranyl *syn*- and *anti*-**1** were chemically stable under an irradiation at 365 nm in an inert atmosphere (Table 2, entry 1). The direct^[36] or photosensitized addition of singlet

oxygen on **1** (*syn* or *anti*) in dichloromethane at 0 °C led to the formation of a mixture of unidentified products (Table 2, entries 2 and 3), instead of the formation of the expected 9,10- or 1,4- endoperoxide. This uncontrolled reactivity probably results from the large steric hindrance on the anthranyl moiety in both *syn*- and *anti*-**1** which leads to the uncontrolled reactivity of ¹O₂, possibly through an intermediate peroxy radical that might then evolve into various oxidation products.

The thermal activation of atropisomers **1** was evaluated under two conditions (Table 2, entry 3). Under neat conditions at 300 °C, *syn*-**1** is isomerized into *anti*-**1**, as already observed for less hindered *ortho*-substituted DPA.^[26b] Interestingly, during these experiments, the compounds partially sublimated. In contrast, when isomers **1** were heated in refluxing C₂H₂Cl₄ (147 °C) in a pressure vial, under argon or air, two new products were cleanly formed: the 9,10-bis-spiro-isobenzofuran-anthracene **4** and a mono-oxidized product **5**. Whatever the relative *syn* or *anti* configuration of the starting material **1**, the products **4** and **5** were isomerized and isolated as a mixture of *syn/anti* isomers. For instance, (±)-*anti*-**1** was transformed into compound (±)-**4** in 35% yield (*syn/anti* ratio = 54:46) and (±)-**5** in 41% yield (*syn/anti* ratio = 51:49). This is thus the first report of a tandem oxidative dearomatization/spirocyclization of substituted anthracenes.

To understand the appearance of ketone **4**, a control experiment was conducted using PhCH(OH)CF₃ in refluxing tetrachloroethane and the slow oxidation into PhCOCF₃ was observed (see the Supporting Information). This oxidation of an aromatic α-trifluoromethyl alcohol thus occurs in the absence

Table 2. Screening for reactivity of bis-trifluoromethyl-alcohols 1 under chemical, light, thermal and oxidative activations. ^[a]			
	Conditions	Reactant	Products (yield) ^[b]
1	Ar, 365 nm	<i>syn</i> - or <i>anti</i> - 1	0% conv.
2	¹ O ₂	<i>syn</i> - or <i>anti</i> - 1	n. d. ^[c]
3	O ₂ , 365 nm	<i>syn</i> - or <i>anti</i> - 1	n. d. ^[c]
4	300 °C, neat	(±)- <i>syn</i> - 1	<i>syn/anti</i> - 1 (18:82)
	reflux, C ₂ H ₂ Cl ₄ ^[d]	(±)- <i>anti</i> - 1	4 (35%) + 5 (41%)
	Bobbitt's salt (excess), 2,6-lutidine, RT, CH ₂ Cl ₂	(<i>R,R</i>) <i>syn</i> - 1	(<i>R,R</i>) <i>syn</i> - 4 (100%)
		(<i>S,S</i>) <i>syn</i> - 1	(<i>S,S</i>) <i>syn</i> - 4 (100%)
		(±)- <i>anti</i> - 1	(±)- <i>anti</i> - 4 (100%)
		(<i>S,S</i>) <i>anti</i> - 1	(<i>S,S</i>) <i>anti</i> - 4 (100%)
5	Magic Blue (2 equiv.), RT, CH ₂ Cl ₂	(<i>R,R</i>) <i>syn</i> - 1	(<i>R,R</i>) <i>syn</i> - 4 (99%)
		<i>meso</i> - <i>syn</i> - 1	<i>meso</i> - <i>syn</i> - 4 (100%)
		(±)- <i>anti</i> - 1	(±)- <i>anti</i> - 4 (100%)
		(<i>R,R</i>) <i>anti</i> - 1	(<i>R,R</i>) <i>anti</i> - 4 (99%)
		<i>meso</i> - <i>anti</i> - 1	<i>meso</i> - <i>anti</i> - 4 (100%)

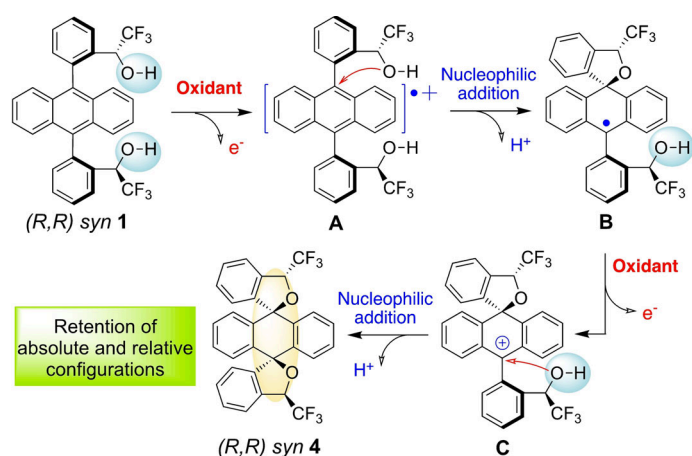
[a] all reactions were conducted with compound **1** in dichloromethane at room temperature, under an argon atmosphere (unless specified) and monitored by thin layer chromatography (TLC) until completion. [b] enantiomeric excess for products **4** are in the range of 99.3–99.8%. [c] not determined (n. d.) as several unidentified compounds were formed. [d] the reaction was conducted in a pressure tube.

of the anthracene moiety and in the presence of residual oxygen.

To control the oxidative dearomatization and avoid thermal isomerization, we investigated the reactivity of **1** in the presence of organic oxidants capable of single-electron transfer (SET) at room temperature (Table 2, entry 4). Bobbitt's oxoammonium salt,^[37] a TEMPO derivative triggered the expected tandem reaction transforming (\pm)-*anti*-**1** exclusively into the bis-spiro-isobenzofuranyl anthracene (\pm)-**4** in 100% yield. To perform the reaction in 24 h, the Bobbitt's reagent was used in excess (10 equiv.) and in the presence of 2,6-lutidine (9 equiv.). Notably, the oxoammonium salt presented an unexpected chemoselectivity towards anthracene, as the reported oxidation of the fluorinated alcohol groups into the corresponding ketone was not observed.^[38]

Even more efficient, the reaction was completed in 1 h using "Magic Blue" (*p*-BrC₆H₄)₃NSbCl₆,^[39] in an exact stoichiometric amount (2 equiv.) and led to bis-spiro-9,9',10,10'-anthracenes **4** in 100% yield, with a retention of relative (*syn/anti*) and absolute stereochemistry (Table 2, entry 4). Importantly, the successful use of these two SET organic oxidants (oxoammonium salt and Magic Blue) represents a new extension of their known ability to functionalize aromatic and polyaromatic compounds such as porphyrinoids.

The proposed mechanism (Scheme 3) for this oxidative dearomatization is a double tandem reaction which consists of a single electron transfer (SET) followed by a nucleophilic addition. The first SET step between the oxidant and the anthracene core affords the corresponding anthranil radical cation **A** that is trapped by an intramolecular nucleophilic addition of one trifluoromethyl-alcohol on position 9, to form 9,9'-spiro anthranil radical **B**, which is probably too hindered to dimerize. The second SET step allows the formation of the stable cation **C**, which again was subjected to the same intramolecular nucleophilic addition of the second alcohol on position 10, offering the bis-spiro dearomatized product **4**.



Scheme 3. Proposed mechanism for the dearomative spirocyclization of anthranil fluorinated alcohols *syn*- and *anti*-**1** (shown: (*R,R*)-*syn*-**1**), with retention of the absolute and relative configurations. This reaction was controlled in the presence of the organic SET oxidants Bobbitt's reagent and Magic Blue in excellent yields (99–100%).

This proposed redox mechanism is fully consistent with the redox potentials of DPA derivatives,^[39] Magic Blue^[40] and TEMPO derivatives^[41] under similar conditions. Concerning the stereochemistry of products **4**, the atropisomerism in **1** maintains the nucleophilic alcohol on its half-space defined by the polyaromatic core, thus ensuring the preservation of relative *syn* or *anti* configuration. The absolute configurations are unchanged, as the reactivity does not involve the two benzylic carbons, in agreement with the proposed mechanism.

The bis-spiro-isobenzofuran anthracenes **4** have shown a remarkable chemical stability. Attempts to open the rings of the spiro-lactone groups under the classical conditions^[18b] for the rearomatization of 9,10-bis-diols-9',10'-dihydroanthracenes with heating (Zn/AcOH, SnCl₂/TFA or KI/AcOH) had no impact on **4**. Indeed, the rearomatization of 9,10-dialkyl-9,10-dimethoxy anthracene derivatives was only described under harsh conditions (alkali metal or TiCl₃/LiAlH₄, 2:1) from robust precursors.^[42]

The double tandem oxidation/spirocyclization of atropisomers **1** provides an attractive alternative oxidative pathway to dearomatize anthracene derivatives, complementary to the well-known cycloadditions and purely ionic tandem reactions. In addition, this access to chiral fluorinated spiro-heterocycles **4** is a complementary route to the rare examples of fluoro-spirocyclizations^[19,20] and post-fluorination of spirocycles.^[21,22]

Chiroptical properties

The access to tunable chiroptical properties is highly desirable to broaden the scope of applications, especially in the fields of detection and materials.^[43] Classically, this is achieved by synthesizing a series of different structures.^[23c,24,44] Recently, several switchable compounds were designed and offered *in-situ* tunable and reversible chiroptical properties thanks to an external stimulus (light, pH, redox or molecular inputs). A third approach consists in designing tunable compounds, whose chiroptical properties can be modified by chemical post-modification. This strategy allows to consider the exploitation of two different chiroptic signatures, from a single compound. As such, the chiroptical properties of enantiopure compounds **1** and the corresponding dearomatized molecules **4** were evaluated to verify the impact of the stereospecific oxidative dearomatization reaction upon anthracene derivatives.

Each pair of enantiomers *syn*-**1** and *anti*-**1** (Figure 4A and B) displayed symmetric circular dichroism (CD) spectra, with opposite Cotton effects. The *syn/anti* relative configuration has no impact upon the CD spectra (see the Supporting Information). Remarkably, the chiroptical response of the anthracene core in the region of 340–400 nm is observed, even if moderate. Despite several bonds separating the anthracene core from the chiral carbon, the 3D architecture of compounds **1** allowed a proximity between both moieties as confirmed by solid state structures. The dimensionless anisotropic ratio $g_{CD} = \Delta\epsilon/\epsilon$ was calculated, with $\Delta\epsilon$ being the differential molar extinction coefficient of left and right circularly polarized light. The obtained g_{CD} factors are around 7.5×10^{-4} on the aromatic and

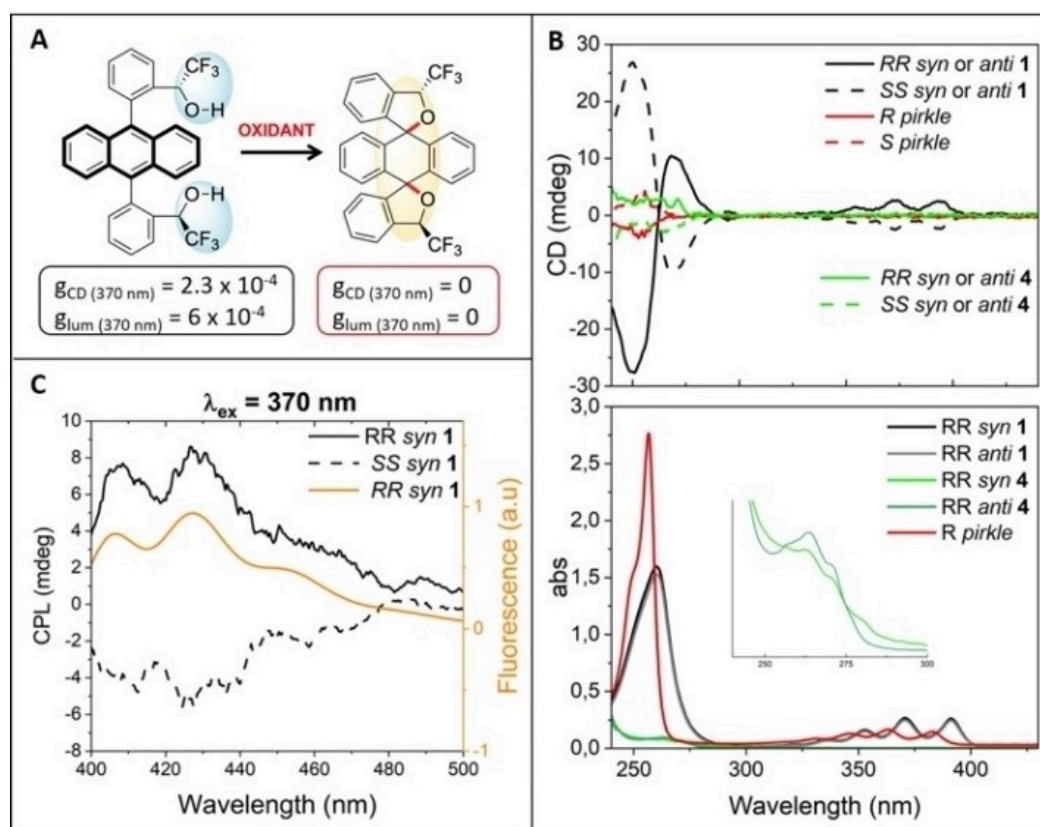


Figure 4. A) Chiroptical properties of enantiopure anthracene derivatives before (compounds **1**) and after (compounds **4**) oxidation; B) UV-Vis. and CD spectra for *syn*-**1** and *syn*-**4**, compared to Pirkle's alcohol. C) Photoluminescence and CPL spectra of enantiopure *syn*-**1** at an excitation wavelength of 370 nm. All spectra were recorded at 17 μM in dichloromethane at 20 °C, under argon.

2.3×10^{-4} on the anthracene moieties (Figure 4A and the Supporting Information). For comparison, Pirkle's alcohol (2,2,2-trifluoro-1-(9-anthryl)ethanol) presented a CD spectrum with a very low intensity without any obvious contribution from the anthranlyl substituent (Figure 4B).

Circularly polarized luminescence (CPL) was detected from enantiomers of **1** upon excitation at 370 nm, which is specific to the anthracene core (Figure 4C). The luminescence dissymmetric factors g_{lum} of *syn*- and *anti*-**1** are about $5\text{--}6 \times 10^{-4}$ ($\lambda_{ex} = 260$ or 370 nm), which are similar to those obtained for small organic discrete polyaromatic compounds, that is, $10^{-5}\text{--}10^{-3}$ (see the Supporting Information).^[45] As seen with CD spectra, these remarkable CPL values arise from the spatial proximity between the emitter (anthracene) and the chiral center (CH(OH)CF₃ group) generated by this controlled atropisomeric architecture.

In comparison, the oxidation products **4** presented weak or absent chiroptical properties. As for Pirkle's alcohol, the CD contribution of the aromatics is very low in the 240–270 nm region and the one corresponding to the anthracene obviously disappears (Figure 4B). For CPL, no g_{lum} was detected for the enantiomers of *syn*-**4** either with an excitation on the aromatics or the anthracene. An obvious quasi extinction of the chiroptical properties (Figure 4B and C) was obtained by a stereospecific oxidative post-modification of **1**.

Conclusion

Novel chiral *syn*- and *anti*-9,10-diphenylanthryl α -trifluoromethyl alcohols have been synthesized. The vicinal arrangement of the groups allows the preferred orientation of the $-\text{CH}(\text{OH})\text{CF}_3$ function in the different quadrants close to the anthracene core depending on the both relative and absolute configurations of each isomer. This structural feature was then exploited to vary the physical properties and reactivity. In the solid state, the compounds self-assemble into H-bonded *syn* homochiral dimers and *anti* ribbons, whereas in chlorinated solvents, they behave as discrete molecules. Taking advantage of the preorganization of anthracene and alcohols groups and their synergic reactivity, the dearomative oxidation of compounds **1** was stereospecifically achieved to 9,10-bis-spiro-isobenzofurananthracene **4** by using organic SET oxidants. The chiroptical properties (CD, CPL) of these α -trifluoromethyl alcohols **1** and the corresponding products **4** were compared and showed an important modulation in intensity. Less demanding in synthesis efforts, this variation of chiroptics by an oxidant stimulus is an attractive way of tuning properties that could be implemented in the future.

Experimental Section

Deposition Numbers 2159931 (*meso-syn-1*), 2159932 (*meso-anti-1*), 2159933 ((\pm) -*syn-1*), 2159949 (*meso-anti-1*.(CH₃COCH₃)), 2159954 ((\pm) -*anti-1*.(DMSO)₃), 2159984 (*meso-anti-4*), 2159985 (*meso-anti-3*), 2159986 ((\pm) -*syn-4*), 2159987 ((\pm) -*syn-3*), 2160002 ((\pm) -*anti-5*), contain the supplementary crystallographic data for this paper. These data are provided free of charge by the joint Cambridge Crystallographic Data Centre and Fachinformationszentrum Karlsruhe Access Structures service.

- [1] For reviews about fluorinated solvents, see: a) J.-P. Bégué, D. Bonnet-Delpon, B. Crousse, *Synlett* **2004**, *1*, 18–29; b) I. Shuklov, N. V. Dubrovina, A. Börner, *Synthesis* **2007**, *19*, 2925–2943; c) J. Wencel-Delord, F. Colobert, *Org. Chem. Front.* **2016**, *3*, 394–400; d) X.-D. An, J. Xiao, *Chem. Rec.* **2020**, *20*, 142–161; e) C. Yu, J. Sanjosé-Orduna, F. W. Patureau, M. H. Pérez-Temprano, *Chem. Soc. Rev.* **2020**, *49*, 1643–1652.
- [2] For recent uses in (photo)redox reactions, see: a) N. E. S. Tay, D. A. Nicewicz, *J. Am. Chem. Soc.* **2017**, *139*, 16100–16104; b) N. Shida, Y. Imada, S. Nagahara, Y. Okada, K. Chiba, *Chem. Commun.* **2019**, *2*, 24; c) S. L. Hooe, E. N. Cook, A. G. Reid, C. W. Machan, *Chem. Sci.* **2021**, *12*, 9733–9741; d) Y. H. Hong, Y.-M. Lee, W. Nam, S. Fukuzumi, *J. Am. Chem. Soc.* **2021**, *144*, 695–700; e) M. Baidya, D. Maiti, L. Roy, S. De Sarkar, *Angew. Chem. Int. Ed.* **2022**, *61*, e202111679.
- [3] I. Colomer, A. E. R. Chamberlain, M. B. Haughey, T. J. Donohoe, *Nat. Chem. Rev.* **2007**, *1*, 0088.
- [4] From refs. [1], the comparison of physical organic properties of TFE, HFIP and ethanol: for the polarity, the Reichart's parameter E_T^N is 0.898 for TFE, 1.068 for HFIP and 0.654 for EtOH; the ionising power Y_{OTs} is 1.8 (TFE), 3.82 (HFIP), –1.75 (EtOH); the pK_a is 12.4 (TFE), 9.3 (HFIP), 15.2 (EtOH), H-bond donating parameter α is 1.51 (TFE), 1.96 (HFIP), 0.83 (EtOH); H-bond accepting parameter β is 0 (TFE, HFIP), and 0.77 (EtOH); nucleophilicity parameter N_{OTs} is –2.78 (TFE), –4.23 (HFIP), 0 (EtOH).
- [5] a) J. Wouters, *Curr. Med. Chem.* **1998**, *5*, 137–162; b) K. Shibatomi, A. Narayama, Y. Abe, S. Iwasa, *Chem. Commun.* **2012**, *48*, 7380–7382; c) I. Erjavec, T. Bordukalo-Niksi, J. Brkljacic, D. Grcevic, G. Mokrovic, M. Rogic, W. Zadadoski, V. M. Paralkar, L. Grgurevic, V. Trkulja, L. Cicin-Sain, S. Vukicevic, *PLoS One* **2016**, *11*, e0150102.
- [6] a) W. H. Pirkle, *J. Am. Chem. Soc.* **1966**, *88*, 1837; b) W. H. Pirkle, M. S. Hoekstra, *J. Am. Chem. Soc.* **1974**, *39*, 3904–3906; c) W. H. Pirkle, T. C. Pochapsky, *Chem. Rev.* **1989**, *89*, 347–362; d) C. Jaime, A. Virgili, R. M. Claramunt, C. Lopez, J. Elguero, *J. Org. Chem.* **1991**, *56*, 6521–6523.
- [7] a) J. Foster, A. L. Pincock, J. A. Pincock, K. A. Thompson, *J. Am. Chem. Soc.* **1998**, *120*, 13354–13361; b) B. Guizzardi, M. Mella, M. Fagnoni, A. Albin, *Chem. Eur. J.* **2003**, *9*, 1549–1554; c) V. Carraminana, A. M. Ochoa de Retana, F. Palacios, J. M. de los Santos, *Molecules* **2020**, *25*, 3332–3358; d) M. Sugiyama, M. Akiyama, K. Nishiyama, T. Okazoe, K. Nozaki, *ChemSusChem* **2020**, *13*, 1775–1784.
- [8] a) M.-F. Ruasse, G. Lo Moro, B. Gallad, R. Bianchini, C. Chiappe, G. Bellucci, *J. Am. Chem. Soc.* **1997**, *119*, 12492–12502; b) H. Mayr, S. Minegishi, *Angew. Chem. Int. Ed.* **2002**, *41*, 4493–4495; *Angew. Chem.* **2002**, *114*, 4674–4676; c) M. Fujita, E. Mishima, T. Okuyama, *J. Phys. Org. Chem.* **2007**, *20*, 241–244; d) A. K. Dhiman, R. Kumar, U. Sharma, *Synthesis* **2021**, *53*, 4124–4130.
- [9] a) M. G. Beaver, K. A. Woerpel, *J. Org. Chem.* **2010**, *75*, 1107–1118; b) S. van der Vorm, H. S. Overkleeft, G. A. van der Marel, J. D. C. Codée, *J. Org. Chem.* **2017**, *82*, 4793–4811.
- [10] a) M. Pérez-Trujillo, I. Maestre, C. Jaime, A. Alvarez-Larena, J. F. Piniella, A. Virgili, *Tetrahedron: Asymmetry* **2005**, *16*, 3084–3093; b) M. Palomino-Schätzlein, A. Virgili, S. Gil, C. Jaime, *J. Org. Chem.* **2006**, *71*, 8114–8120; c) J. Mendizabal, P. de March, J. Recasens, A. Virgili, A. Alvarez-Larena, J. Elguera, I. Alkorta, *Tetrahedron* **2012**, *68*, 9645–9651.
- [11] a) M. Omote, A. Kominato, M. Sugawara, K. Sato, A. Ando, I. Kumadaki, *Tet. Lett.* **1999**, *40*, 5583–5585; b) T. Katagiri, Y. Fujiwara, S. Takahashi, N. Osaki, K. Uneyama, *Chem. Commun.* **2002**, 986–987; c) Y. S. Sokeirik, M. Omote, K. Sato, I. Kumadaki, A. Ando, *Tetrahedron: Asymmetry* **2006**, *17*, 2654–2658; d) S. Lauzon, T. Ollevier, *Chem. Commun.* **2021**, *57*, 11025–11028.
- [12] a) A. Shokri, X.-B. Wang, S. R. Kass, *J. Am. Chem. Soc.* **2013**, *135*, 9535–9530; b) M. Samet, M. Danesh-Yazdi, A. Fattahi, S. R. Kass, *J. Org. Chem.* **2015**, *80*, 1130–1135.
- [13] a) C. Houle, P. R. Savoie, C. Davies, D. Jardel, P. A. Champagne, B. Bibal, J.-F. Paquin, *Chem. Eur. J.* **2020**, *26*, 10620–10625.
- [14] For a selection, see: a) A. Berkessel, S. S. Vormittag, N. E. Schlörner, J.-M. Neudörfl, *J. Org. Chem.* **2012**, *77*, 10145–10157; b) A. Berkessel, J. Krämer, F. Mummy, J.-M. Neudörfl, R. Haag, *Angew. Chem. Int. Ed.* **2013**, *52*, 739–743; *Angew. Chem.* **2013**, *125*, 767–771.
- [15] a) A. Berkessel, J. A. Adrio, D. Hüttenhaim, J.-M. Neudörfl, *J. Am. Chem. Soc.* **2006**, *128*, 8421–8426; b) O. Holloczki, A. Berkessel, J. Mars, M. Mezger, A. Wiebe, S. R. Waldvogel, B. Kirchner, *ACS Catal.* **2017**, *7*, 1846–1852.
- [16] For recent examples of chiral atropisomers with two stereogenic center/axis at least, see: a) K. T. Barrett, A. J. Metrano, P. R. Rablen, S. J. Miller, *Nature* **2014**, *509*, 71–75; b) X. Bao, J. Rodriguez, D. Bonne, *Chem. Sci.* **2020**, *11*, 403–408; c) X. Bao, J. Rodriguez, D. Bonne, *Angew. Chem. Int. Ed.* **2020**, *59*, 12623–12634 and references herein; d) L. Jin, P. Zhang, Y. Li, X. Yu, B.-F. Shi, *J. Am. Chem. Soc.* **2021**, *143*, 12335–12344.
- [17] a) U. Svanholm, V. D. Parker, *J. Chem. Soc. Perkin Trans. 2* **1976**, 1567–1574; b) J. O. Howell, R. M. Wightman, *J. Phys. Chem.* **1984**, *88*, 3918–3920.
- [18] a) W. C. Wertjes, E. H. Southgate, D. Sarlah, *Chem. Soc. Rev.* **2018**, *47*, 7996–8017; b) J. L. Marshall, D. Lehnher, B. D. Lindner, R. R. Tykwinski, *ChemPlusChem* **2017**, *82*, 967–1001.
- [19] For reviews about fluorocyclizations, see: a) S. C. Wilkinson, R. Salmon, V. Gouverneur, *Future Med. Chem.* **2009**, *1*, 847–863; b) J. R. Wolstenhulme, J. Rosenqvist, O. Lozano, J. Ilupeju, N. Wurz, K. M. Engle, G. W. Pidgeon, P. R. Moore, G. Sandford, V. Gouverneur, *Angew. Chem. Int. Ed.* **2013**, *52*, 9796–9800; *Angew. Chem.* **2013**, *125*, 9978–9982; c) D. Parmar, M. Rieping, *Chem. Commun.* **2014**, *50*, 13928–13931; d) X.-G. Hu, L. Hunter, *Beilstein J. Org. Chem.* **2013**, *9*, 2696–2708; e) Y. A. Sergucheve, M. V. Ponomarenko, N. V. Ignat'ev, *J. Fluor. Chem.* **2016**, *185*, 1–16.
- [20] a) J.-H. Ye, L. Song, W.-J. Zhou, T. Ju, Z.-B. Yin, S.-S. Yan, Z. Zhang, J. Li, D.-G. Yu, *Angew. Chem. Int. Ed.* **2016**, *55*, 10022–10026; *Angew. Chem.* **2016**, *128*, 10176–10180; b) J.-H. Ye, L. Zhu, S.-S. Yan, M. Miao, X.-C. Zhang, W.-J. Zhou, J. Li, Y. Lan, D.-G. Yu, *ACS Catal.* **2017**, *7*, 8324–8330.
- [21] K. Fjellbye, M. Marigo, R. P. Clausen, K. Juhl, *Synlett* **2017**, *28*, 425–428.
- [22] A photo-induced dearomative oxidation of *gem*-difluoroindoles was described without stereocontrol: Q. Wang, Y. Qu, Q. Xia, H. Song, H. Song, Y. Liu, Q. Wang, *Chem. Eur. J.* **2018**, *24*, 11283–11287.

- [23] For recent examples of tuning chiroptics by using series of compounds, see: a) G. Liu, C. Zhou, W. L. Teo, C. Qian, Y. Zhao, *Angew. Chem. Int. Ed.* **2019**, *58*, 9366–9372; *Angew. Chem.* **2019**, *131*, 9466–9472; b) J.-K. Li, X.-Y. Chen, Y.-L. Guo, X.-C. Wang, A. C.-H. Sue, X.-Y. Cao, X.-Y. Wang, *J. Am. Chem. Soc.* **2021**, *143*, 17958–17963; c) V. Zullo, A. Iuliano, G. Pescitelli, F. Zinna, *Chem. Eur. J.* **2022**, *28*, e202104226.
- [24] A representative example of tuning chiroptics by post-modification: L. Norel, M. Rudolph, N. Vanthuynne, J. A. G. Williams, C. Lescop, C. Roussel, J. Autschbach, J. Crassous, R. Réau, *Angew. Chem. Int. Ed.* **2010**, *49*, 99–102; *Angew. Chem.* **2010**, *122*, 103–106.
- [25] M. Cayla, D. Sonet, E. Tarayre, R. Bapt, B. Bibal, unpublished results.
- [26] a) D. Zehm, W. Fudickar, T. Linker, *Angew. Chem. Int. Ed.* **2007**, *46*, 7689–7692; *Angew. Chem.* **2007**, *119*, 7833–7836; b) D. Zehm, W. Fudickar, M. Hans, U. Schilde, A. Kelling, T. Linker, *Chem. Eur. J.* **2008**, *14*, 11429–11441.
- [27] For atropisomeric molecular triads based on smaller aromatic compounds than anthracene, see: a) J. Gawronski, K. Kacprzak, *Chirality* **2002**, *14*, 689–702; b) C. Roussel, R. Kaid-Slimane, F. Andreoli, M. Renaudin, N. Vanthuynne, *Chirality* **2009**, *21*, 160–166; c) J.-Y. Wang, Y. Tang, G.-Z. Wu, S. Zhang, H. Rouh, S. Jin, T. Xu, Y. Wang, D. Unruh, K. Surowiec, Y. Ma, Y. Li, C. Katz, H. Liang, W. Cong, G. Li, *Chem. Eur. J.* **2022**, *28*, e202104102.
- [28] a) N. Duangdee, W. Harnying, G. Rulli, J.-M. Neudörfl, H. Gröger, A. Berkessel, *J. Am. Chem. Soc.* **2012**, *134*, 11196–11205; b) R. P. Singh, J. M. Shreeve, *J. Fluorine Chem.* **2012**, *133*, 20–26.
- [29] a) J. T. Edward, *J. Chem. Educ.* **1970**, *47*, 261–270; b) Y. Cohen, L. Avram, L. Frisch, *Angew. Chem. Int. Ed.* **2005**, *44*, 520–554; *Angew. Chem.* **2005**, *117*, 524–560.
- [30] W. Bauer, *Magn. Reson. Chem.* **1996**, *34*, 532–537.
- [31] a) M. Pomares, F. Sanchez-Ferrando, A. Virgili, A. Alvarez-Larena, J. F. Piniella, *J. Org. Chem.* **2002**, *67*, 753–758; b) A. Mazzanti, A. Drakopoulos, T. Christina, A. Kolocouris, *ChemistrySelect* **2019**, *4*, 7645–7648.
- [32] a) H. Meir, D. Cao, *Chem. Soc. Rev.* **2013**, *42*, 143–155; b) R. Remy, C. G. Bochet, *Chem. Rev.* **2016**, *116*, 9816–9849.
- [33] J. C. C. Atherton, S. Jones, *Tetrahedron* **2003**, *59*, 9039–9057.
- [34] F. Lopez Ortiz, M. J. Iglesias, I. Fernandez, C. M. Andujar Sanchez, G. Ruiz Gomez, *Chem. Rev.* **2007**, *107*, 1580–1691.
- [35] A. Velian, C. C. Cummins, *J. Am. Chem. Soc.* **2012**, *134*, 13978–13981, and references therein.
- [36] For the photosensitization of dioxygen by DPA, see: A. K. Gupta, K. K. Rohatgi-Mukherjee, *Photochem. Photobiol.* **1978**, *27*, 539–543.
- [37] a) J. M. Bobbitt, *J. Org. Chem.* **1998**, *63*, 9367–9374; b) H. Richter, R. Fröhlich, C.-G. Daniliuc, O. Garcia Mancheno, *Angew. Chem. Int. Ed.* **2012**, *51*, 8656–8660; *Angew. Chem.* **2012**, *124*, 8784–8788; c) L. Tebben, A. Studer, *Angew. Chem. Int. Ed.* **2011**, *50*, 5034–5068; *Angew. Chem.* **2011**, *123*, 5138–5174.
- [38] C. B. Kelly, M. A. Mercandante, T. A. Hamlin, M. H. Fletcher, N. E. Leadbeater, *J. Org. Chem.* **2012**, *77*, 8131–8141.
- [39] a) C. M. Davis, K. Ohkubo, I. T. Ho, Z. Zhang, M. Ishida, Y. Fang, V. M. Lynch, K. M. Kadish, J. L. Sessler, S. Fukuzumi, *Chem. Commun.* **2015**, *51*, 6757–6760; b) J. A. Christensen, B. T. Phelan, S. Chaudhuri, A. Acharya, V. S. Batista, M. R. Wasielewski, *J. Am. Chem. Soc.* **2018**, *140*, 5290–5299; c) C. Li, Q. Li, J. Shao, Z. Tong, M. Ishida, G. Baryshnikov, H. Agren, H. Furuta, Y. Xie, *J. Am. Chem. Soc.* **2020**, *142*, 17195–17205.
- [40] a) M. M. Sartin, C. Shu, A. J. Bard, *J. Am. Chem. Soc.* **2008**, *130*, 5354–5360; b) N. G. Connelly, W. E. Geiger, *Chem. Rev.* **1996**, *96*, 877–910; c) J. Ichikawa, H. Tanabe, S. Yoshida, T. Kawai, M. Shinjo, T. Fujita, *Chem. Asian J.* **2013**, *8*, 2588–2591.
- [41] J. E. Nutting, M. Rafiee, S. S. Stahl, *Chem. Rev.* **2018**, *118*, 4834–4885.
- [42] a) H. M. Walborsky, H. H. Wüst, *J. Am. Chem. Soc.* **1982**, *104*, 5807–5808; b) M. Quernheim, F. E. Golling, W. Zhang, M. Wagner, H.-J. Räder, T. Nishiuchi, K. Müllen, *Angew. Chem. Int. Ed.* **2015**, *54*, 10341–10346; *Angew. Chem.* **2015**, *127*, 10482–10487; c) E. S. Hirst, R. Jasti, *J. Org. Chem.* **2012**, *77*, 10473–10478.
- [43] For some reviews, see: a) J. W. Canary, S. Mortezaei, J. Liang, *Coord. Chem. Rev.* **2010**, *254*, 2249–2266; b) J. OuYang, J. Crassous, *Coord. Chem. Rev.* **2016**, *376*, 533–547; c) L. Zhang, H.-X. Wang, S. Li, M. Liu, *Chem. Soc. Rev.* **2020**, *49*, 9095–9120.
- [44] J.-K. Li, X.-Y. Chen, Y.-L. Guo, X.-C. Wang, A. C.-H. Sue, X.-Y. Cao, X.-Y. Wang, *J. Am. Chem. Soc.* **2021**, *143*, 17958–17963.
- [45] a) E. M. Sanchez-Carnerero, A. R. Agarrabeitia, F. Moreno, B. L. Maroto, G. Muller, M. J. Ortiz, S. de la Moya, *Chem. Eur. J.* **2015**, *21*, 13488–13500; b) J. Kumar, T. Nakashima, T. Kawai, *J. Phys. Chem. Lett.* **2015**, *6*, 3445–3452; c) J. Liu, H. Su, L. Meng, Y. Zhao, C. Deng, J. C. Y. Ng, P. Lu, M. Faisal, J. W. Y. Lam, X. Huang, H. Wu, K. S. Wong, B. Z. Tang, *Chem. Sci.* **2012**, *3*, 2737–2747.